Hydrothermal synthesized porous Co(OH)$_2$ nanoflake film for supercapacitor application

ZHANG YongQi, XIA XinHui, KANG Jing & TU JiangPing[*]

State Key Laboratory of Silicon Materials and Department of Materials Science and Engineering, Zhejiang University, Hangzhou 310027, China

Porous Co(OH)$_2$ film directly grown on nickel foam is prepared by a facile hydrothermal method. The as-prepared Co(OH)$_2$ film possesses a structure consisting of randomly porous nanoflakes with thicknesses of 20–30 nm. The capacitive behavior of the Co(OH)$_2$ film is investigated by cyclic voltammograms and galvanostatic charge-discharge tests in 2 mol/L KOH. The porous Co(OH)$_2$ film exhibits a high discharge capacitance of 935 F g^{-1} at a current density of 2 A g^{-1} and excellent rate capability. The specific capacitance keeps a capacitance of 589 F g^{-1} when the current density increases to 40 A g^{-1}. The specific capacitance of 82.6% is maintained after 1500 cycles at 2 A g^{-1}.

supercapacitor, Co(OH)$_2$ film, electrochemical property, hydrothermal method

Supercapacitors, also called electrochemical capacitors (ECs), have attracted great attention due to their fast recharge ability, high power performance, long cycle life and environment-friendly merit. As an emerging energy storage device, ECs have shown the potential to combine the high energy density of conventional batteries and the high power density of electrostatic capacitors [1–3]. With respect to electrode materials, there are three main categories: carbon-based, transition metal oxides/hydroxides and conductive polymers [2,4,5]. Dependent upon the charge-storage mechanism, electrochemical capacitors can be divided into electrical double-layer capacitors (EDLCs) and pseudo-capacitors concerning reversible redox reactions [2].

Pseudocapacitive materials, such as transition metal oxides/hydroxides and conducting polymers, are being explored for producing supercapacitors with increased specific capacitances (several times larger than those of carbonaceous materials) and high energy densities [2–6]. RuO$_2$-base electrode materials are well studied as pseudo-capacitive electrode materials with remarkable performance

(760 F g^{-1} for a single electrode system) [7]. However, apart from being toxic, RuO$_2$ is quite expensive for extensive commercial applications. Therefore, great efforts have been devoted to searching for inexpensive alternative transition metal oxides/hydroxides materials with good capacitive characteristics [8–17]. Co(OH)$_2$ is an attractive pseudo-capacitive material because of its high specific capacitance, well-defined electrochemical redox activity, and low cost [14,15]. A nano-level whisker-like Co(OH)$_2$ powder was fabricated by Yuan's group [15] and showed excellent electrochemical performance. On the other hand, it is well accepted that pseudo-capacitance is an interfacial phenomenon tightly related to the morphology of electroactive materials. The porous structure could provide a very short diffusion pathway for ions as well as large active surface area, leading to enhanced electrochemical properties [2,3,5]. Compared to powder, the film structure materials have good conductivity under the same conditions.

In the present work, the porous Co(OH)$_2$ nanoflake film on nickel foam is prepared by hydrothermal method. Remarkably, the as-prepared film exhibits superior performances with excellent capacity retention and high specific

*Corresponding author (email: tujp@zju.edu.cn)

capacitance during cycling.

1 Experimental

(i) Chemical materials. The cobalt nitrate $[Co(NO_3)_2 \cdot 6(H_2O)]$, hexamethylenetetramine $(C_6H_{12}N_4)$ and potassium hydroxide were analytical grade and were used without further purification. All aqueous solutions were freshly prepared with deionized water. Nickel foam substrate with a size of 2 cm × 3 cm was cleaned ultrasonically in ethanol for 10 min. Its top side was protected for solution contamination by uniformly coating with a polytetrafluoroethylene tape.

(ii) Prepareation of porous $Co(OH)_2$ nanoflake film. The reaction bath for the deposition of $Co(OH)_2$ contained 0.1 mol L^{-1} $Co(NO_3)_2 \cdot 6(H_2O)$, and 0.05 mol/L $C_6H_{12}N_4$. The cleaned nickel foam substrates were immersed vertically in the deposition bath. Deposition was carried out at 90°C for 5 h. After the deposition, the films were immersed in deionized water and then dried in air. The average loading is determined to be 4.3 mg cm^{-2}, which is calculated by measuring the nickel foam substrate before and after the deposition via a DENVER TB-25 analytical balance.

(iii) Characterization. The structure and morphology of the film were characterized by X-ray diffraction (XRD, PANalytical/X'Pert PRO), scanning electron microscopy (SEM, Philips-FEI/SIRION-100). Electrochemical measurements were carried out in a three-electrode electrochemical cell containing 2 mol/L KOH aqueous solution as the electrolyte. Electrochenmical measurements were performed on a CHI660c electrochemical workstation (Chenhua, Shanghai) at room temperature, with the porous $Co(OH)_2$ film as the working electrode, Hg/HgO as the reference electrode and a Pt foil as the counter electrode.

2 Results and discussion

2.1 Synthesis and characterization of porous $Co(OH)_2$ nanoflake film

The XRD pattern of the porous $Co(OH)_2$ nanoflake film on nickel foam substrate is shown in Figure 1. With the exclusion of three strong peaks from the nickel foam substrate, the XRD pattern depicts reflections at 2θ values of 11.6°, 19.5°, 33.2° and 59.0°, which can be indexed as (001), (002), (100) and (110) crystal planes of α-$Co(OH)_2$ phase (JCPDS 74-1057), respectively. The diffraction peak at 11.6° indexed to (001) plane of α-$Co(OH)_2$ is much stronger than the others. It implies that the preferable growth of α-$Co(OH)_2$ along (001) direction.

Figure 2 shows typical SEM images of the nickel foam substrate and the porous $Co(OH)_2$ film. The nickel foam substrate shows a three-dimensional cross-linked structure
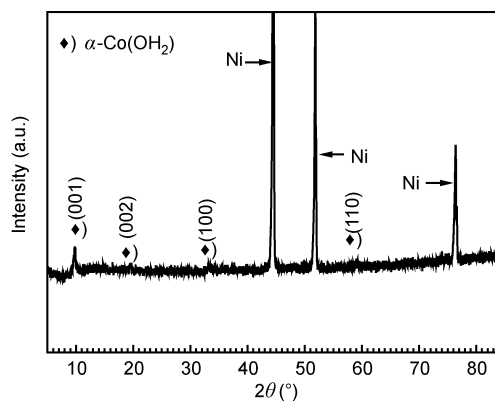

**Figure 1**   XRD pattern of the porous $Co(OH)_2$ film.

with considerable grids on its surface (Figure 2(a)). The magnified image shows that the skeleton of nickel foam is dense and smooth (Figure 2(b)). The $Co(OH)_2$ thin film exhibits a highly porous net-like structure constructed of many interconnected nanoflakes with thicknesses of 20–30 nm. The nanoflakes are arranged vertically to the substrate, forming a net-like structure and leaving pores of 30–300 nm. The macropores in the porous $Co(OH)_2$ nanoflake film can absorb and strongly retain electrolyte ions, ensuring sufficient faradic reactions, especially at high current densities. The net-like porous superstructure can afford high specific surface area for electrochemical energy storage. Thus, it is believed that this hierarchically porous structure is beneficial to the enhancement of pseudocapacitive performance.

2.2 Electrochemical measurements

Figure 3(a) shows the first ten CV curves of $Co(OH)_2$ film electrode at a scan rate of 10 mV s^{-1} between 0 and 0.6 V (vs. Hg/HgO). The CV curves exhibit two redox couples: $P_1(0.3$ V)/P_2 (0.45 V) and P_3 (0.55 V)/P_4 (0.25 V), instead of ideal rectangular shape. The first redox couple P_1/P_2 corresponds to the conversion between $Co(OH)_2$ and CoOOH, which can be simply expressed as

$$Co(OH)_2 + OH^- \leftrightarrow CoOOH + H_2O + e^- \qquad (1)$$

The redox couple P_3/P_4 is due to the change between CoOOH and CoO_2, represented by the following reaction:

$$CoOOH + OH^- \leftrightarrow CoO_2 + H_2O + e^- \qquad (2)$$
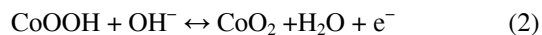
The charge process of the electrode is associated with the oxidation peak, whereas the discharge process is associated with the reduction peak. It indicates that the capacity mainly results from the pseudo-capacitance, which is based on a redox mechanism. After the fifth cycle, the CV curves match almost exactly, which implies the system has reached a steady state. Figure 4 shows the *ex-situ* XRD pattern of the porous $Co(OH)_2$ film electrode charged to 0.6 V after CV measurement. From the XRD pattern, it can only observe the diffraction peaks of CoOOH. Maybe the CoO_2
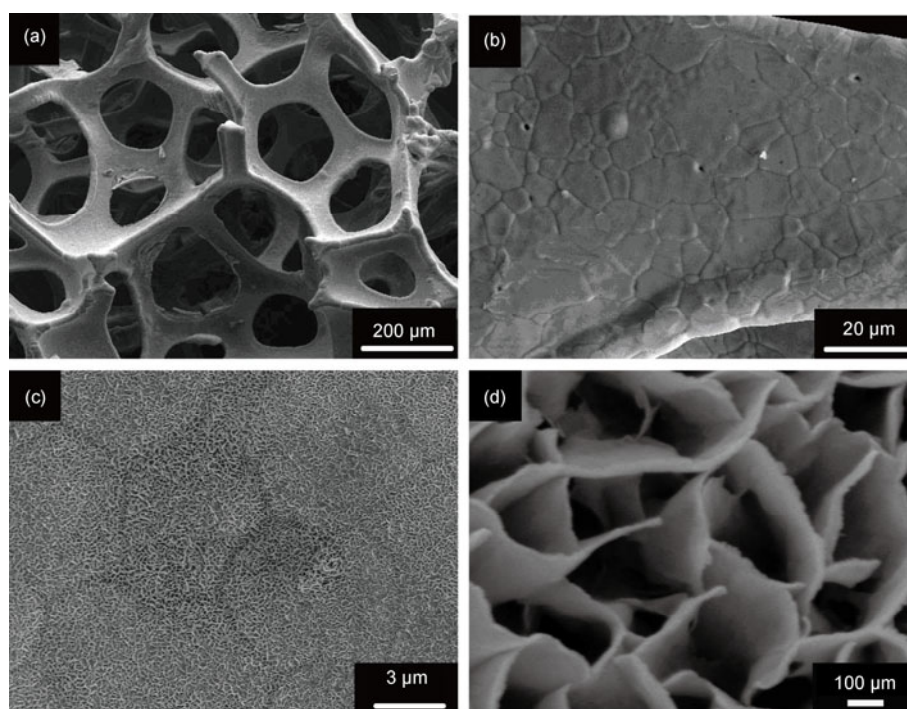
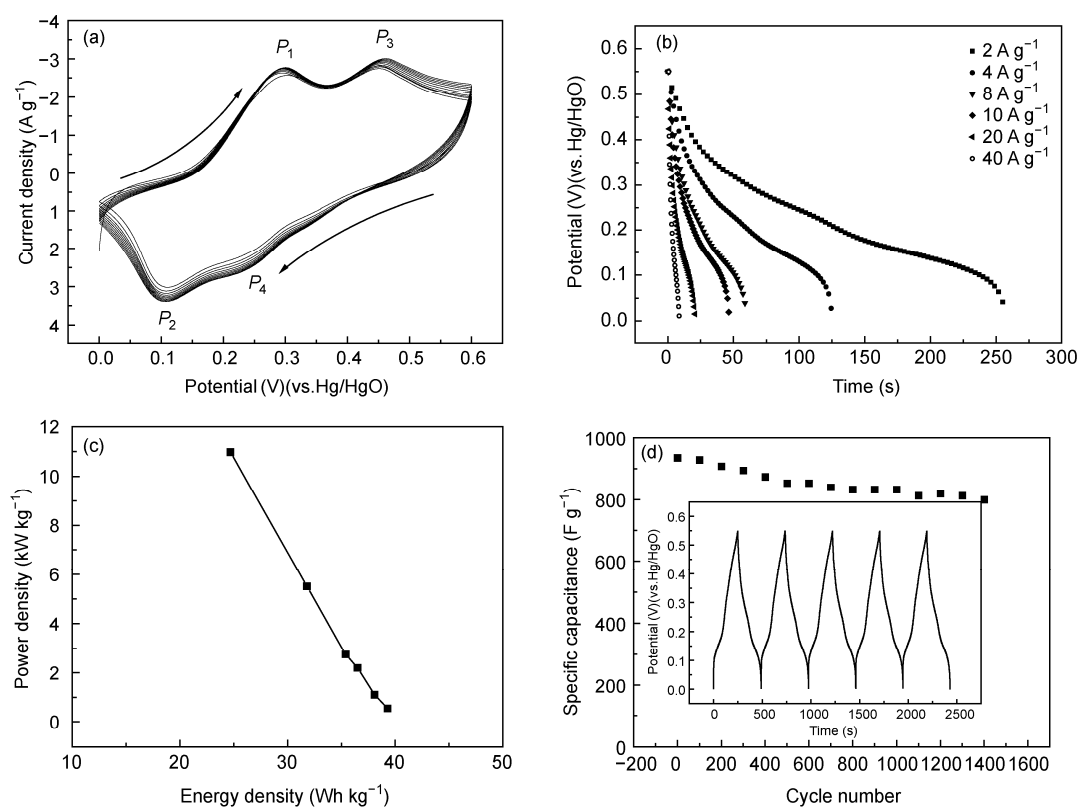**Figure 2**   SEM images of Ni substrate and the porous Co(OH)₂ film.

Figure 3   Electrochemical characterizations of the porous Co(OH)₂ film. (a) CV curves at scan rates of 10 mV s⁻¹; (b) discharge curves at different discharge current densities; (c) Ragone plots (power density vs. energy density); (d) cycling performances of the porous Co(OH)₂ film at 2 A g⁻¹ (the inset is the charge/discharge curves of the porous Co(OH)₂ film).
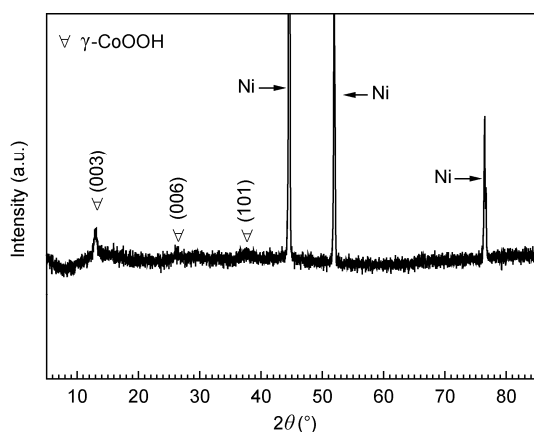
Figure 4 *Ex-situ* XRD pattern of the porous $Co(OH)_2$ film after charging to 0.6 V.

phase is unstable in air. This phenomenon requires further study.

In practice, the ability to discharge at high rate is crucial in capacitors. The specific capacitances are calculated from the discharge curves using the following equation:

$$C = \frac{I\Delta t}{m\Delta V},$$ (3)

where C (F g^{-1}) is specific capacitance, I (mA) represents the current applied and m (mg), ΔV (V) and Δt (s) designate the mass of the active materials, potential drop during discharge and total discharge time, respectively. Figure 3(b) shows the pseudo-capacitances of the porous $Co(OH)_2$ nanoflake film at different discharge current densities are elucidated by galvanostatic charge-discharge tests in the potential range of 0 to 0.55 V (vs. Hg/HgO) (charge current density is 2 A g^{-1}). In this way, the specific capacitance of the porous $Co(OH)_2$ nanoflake film electrode at a galvanostatic current density of 2, 4, 8, 10, 20 and 40 A g^{-1} are 935, 908, 870, 842, 756 and 589 F g^{-1}, respectively. With the current density increasing, partial active materials have no time to react, leading to the specific capacitance decrease [12,18]. The 63% of capacitance is retained when the current density changes from 2 to 40 A g^{-1}. The results show that the porous $Co(OH)_2$ nanoflake film electrode processes excellent rate capacity.

The energy density E (Wh kg^{-1}) and power density P (W kg^{-1}) are also important factors required for practical applications.

$$E = \frac{CU^2}{2m},$$ (4)

$$P = \frac{UI}{m},$$ (5)

where C (F) is the specific capacitance, U (V) is the voltage applied on the cell, I (A) represents the current applied and m (kg) designates the mass of the active materials. The en-

ergy and power densities are derived from the discharge curves of the electrode at different discharge current densities using eqs. (4) and (5). The Ragone plot (power density vs. energy density) shows that the electrode delivered a high energy density of about 24.7 Wh kg^{-1} at a high power density of 11 kW kg^{-1} (Figure 3(c)).

Figure 3(d) shows the cyclability of the porous $Co(OH)_2$ nanoflake film electrode over 1500 cycles between 0 and 0.55 V at a charge-discharge current density of 2 A g^{-1}. The porous $Co(OH)_2$ nanoflake film has a specific capacitance of 772 F g^{-1}, pseudocapacitance retention of 82.6% after 1500 cycles, indicating excellent cycling stability. Importantly, the columbic efficiency was nearly 100% through the charge/discharge curves of the $Co(OH)_2$ electrode (inset in Figure 3(b)). The excellent electrochemical performance is mainly attributed to the following two reasons. First, the porous structure provides a large specific surface area for electrolyte access and shortens the diffusion path in solid phase, resulting in fast redox reactions. Second, every nanofake grows directly on the foam nickel substrate, which can enhance the conductivity of the electrode.

3 Conclusion

In summary, a porous $Co(OH)_2$ film, consisting of randomly porous nanoflakes with thicknesses of 20 nm and directly grown on nickel foam is prepared by a facile hydrothermal method. The porous $Co(OH)_2$ film exhibits a high discharge capacitance of 935 F g^{-1} at 2 A g^{-1} and excellent rate capability. The excellent electrochemical capacitive performance is mainly due to the high porosity and large surface area of the porous architecture. It is believed that porous $Co(OH)_2$ film has promising applications for supercapacitor.

1 Conway B E. Transition from "supercapacitor" to "battery" behavior in electrochenmical energy storage. J Electrochem Soc, 1991, 138: 1539–1548
2 Simon P, Gogotsi Y. Materials for electrochemical capacitors. Nat Mater, 2008, 7: 845–854
3 Miller J R, Simon P. Electrochemical capacitors for energy management. Science, 2008, 321: 651–652
4 Sarangpani S, Tilak B V, Chen C P. Materials for electrochemical capacitors. J Electrochem Soc, 1996, 143: 3791–3796
5 Zhang Y, Feng H, Wu X B, et al. Progress of electrochemical capacitor electrode materials: A review. Int J Hydrogen Energ, 2009, 34: 4889–4899
6 Li F, Shi J J, Qin X. Synthesis and supercapacitor characteristics of PANI/CNTs composites. Chin Sci Bull, 2010, 55: 1100–1106
7 Zheng J P, Cygan P J, Jow T R. Hydrous ruthenium oxide as an electrode material for electrochemical capacitors. J Electrochem Soc, 1995, 142: 2699–2703
8 Wang H, Casalongue H S, Liang Y. Ni(OH)₂ nanoplates grown on graphene as advanced electrochemical pseudocapacitor materials. J Am Chem Soc, 2010, 132: 7472–7477

9   Kim J H, Zhu K, Yan Y F, et al. Microstructure and pseudocapacitive properties of electrodes constructed of oriented NiO-TiO$_2$ nanotube arrays. Nano Lett, 2010, 10: 4099–4104

10 Wang D W, Li F, Cheng H M. Hierarchical porous nickel oxide and carbon as electrode materials for asymmetric supercapacitor. J Power Sources, 2008, 185: 1563–1568

11 Ahn H J, Kim W B, Seong T Y. Co(OH)$_2$-combined carbon-nanotube array electrodes for high-performance micro-electrochemical capacitors. Electrochem Commun, 2008, 10: 1284–1287

12 Zhou W J, Zhang J, Xue T, et al. Electrodeposition of ordered mesoporous cobalt hydroxide film from lyotropic liquid crystal media for electrochemical capacitors. J Mater Chem, 2008, 18: 905–910

13 Wang X, Yuan A, Wang Y. Supercapacitive behaviors and their temperature dependence of sol-gel synthesized nanostructured manganese dioxide in lithium hydroxide electrolyte. J Power Sources, 2007, 172: 1007–1011

14 Xia X H, Tu J P, Wang X L, et al. Mesoporous Co$_3$O$_4$ monolayer hollow-sphere array as electrochemical pseudocapacitor material. Chem Commun, 2011, 47: 5786–5788

15 Yuan C Z, Hou L R, Shen L F, et al. A novel method to synthesize whisker-like Co(OH)$_2$ and its electrochemical properties as an electrochemical capacitor electrode. Electrochim Acta, 2010, 56: 115–121

16 Cao L, Zhou Y K, Lu M, et al. Preparation of nanocrystalline Co$_3$O$_4$ and its properties as supercapacitors. Chin Sci Bull, 2003, 48: 1212–1215

17 Yu W P, Yang X P, Wang G M. A study on nano-sized NiO electrodes doping with C and Co prepared by electrochemical deposition sintering processes and their capacitance performance. Chin Sci Bull, 2004, 49: 1446–1449

18 Kong L B, Liu M C, Lang J W. Porous cobalt hydroxide film electrodeposited on nickel foam with excellent electrochemical capacitive behavior. J Solid State Electrochem, 2011, 15: 571–577